J. Mol. Biol. (1987) **194**, 299–312

Recombination of Carbon Monoxide to Ferrous Horseradish Peroxidase Types A and C

Wolfgang Doster†, Samuel F. Bowne‡, Hans Frauenfelder Lou Reinisch§ and Erramilli Shyamsunder‖

Department of Physics
University of Illinois at Urbana-Champaign
1110 West Green Street, Urbana, IL 61801, U.S.A.

(Received 8 April 1986, and in revised form 9 October 1986)

The recombination of carbon monoxide to isoenzymes A2 and C of horseradish peroxidase (HRP) was studied as a function of temperature (2 to 320 K) and pH (5 to 8·3) with flash photolysis and infrared difference absorption. At low temperatures three geminate recombination processes are observed. One of these internal processes, denoted by I*, is exponential in time with a rate coefficient that deviates strongly from an Arrhenius behavior below 100 K, implying phonon-assisted tunneling. The two other processes, denoted by I, are non-exponential in time and related to different carbonyl isomers, as shown by the infrared difference spectra. The existence of three internal processes indicates that HRP differs considerably from myoglobin where only one internal process, I, is seen. Moreover, the internal processes in HRP are faster than process I in myoglobin. At 300 K, only one recombination process from the solvent is observed and it is very slow ($\lambda_S \approx 1\ s^{-1}$ at 1 atm CO (1 atm = 101,325 Pa)), much slower than the corresponding association process in myoglobin. Since process I is fast, but binding from the solvent is slow, the barrier at the heme cannot be responsible for the small association rate. The infrared absorption difference spectra of the amide I/II bands indicate that photolysis and recombination trigger a two-step structural change. The slow recombination rate at 300 K can thus be explained by the large Gibbs energy of the conformational transition that is necessary to let CO move into the heme pocket. The partition coefficient for the CO in the heme pocket and the solvent is extremely small, while bond formation with the heme iron occurs in less than 100 nanoseconds.

1. Introduction

Peroxidases and catalases are heme proteins like hemoglobin, myoglobin and the cytochromes. Unlike hemoglobin and myoglobin, however, they are enzymes. Horseradish peroxidase (HRP; M_r 44,000; EC 1.11.1.7)¶ contains the iron protoporphyrin type IX and a co-ordinated histidine in the fifth position like hemoglobin and myoglobin. In its ferrous state, HRP forms compounds with CO, NO, CN and RCN, with spectral properties similar to those of hemoglobin and myoglobin, but its reactions with hydrogen peroxide and oxygen are different (Brill *et al.*, 1966). At room temperature CO binds to HRP about 10^3 times slower than to myoglobin (Mb); Kertez *et al.* 1965). Yamasaki *et al.* (1978) attributed the differences to a stronger interaction of the distal histidine, the heme-linked ionizing group, with the CO. (The term heme-linked was introduced by Yamasaki *et al.* (1978) to denote a group that is functionally linked to the heme without necessarily being covalently bound to the heme.) Alternatively, Mincey & Taylor (1980) suggested ionization of the proximal histidine. LaMar *et al.* (1982) demonstrated, however, that the proximal histidine is protonated

† Technische Universität München, Physik-Department E-13, D-8046 Garching, F.R.G.
‡ University of California, Department of Molecular Biology, Berkeley, CA 94720, U.S.A.
§ Northeastern University, Department of Physics, Boston, MA 02115, U.S.A.
‖ Princeton University, Department of Physics, Princeton, NJ 08544, U.S.A.

¶ Abbreviations used: HRP, horseradish peroxidase; Mb, myoglobin; i.r., infrared; cm-cyt *c*, carboxymethylated cytochrome *c*; n.m.r., nuclear magnetic resonance.

0022-2836/87/060299-14 $03.00/0

even at high pH. Resonance Raman spectra indicate a pH-dependent frequency shift of the iron-proximal histidine stretching mode, which cannot be due to the deprotonation of the proximal histidine (Teraoka & Kitagawa, 1981). No such frequency shift is observed in Mb. The pH dependence of the Raman band in HRP is assumed to be due to the deprotonation of the distal histidine, communicated to the Fe–N^{ε} (proximal histidine) bond *via* the globin. It is of interest to study how these molecular differences in the heme environment, the strength of the iron–histidine bond, and the interaction of the heme with its distal base affect the kinetics of CO binding.

In this paper, we describe the reaction of carbon monoxide with two plant peroxidases, types A2 and C. In the reduced state, A2 and C have different acid–base properties, with pK_a values of 5·5 and 7, respectively. It has been suggested that stabilization of the imidazolium ion of the distal histidine by an anion is stronger in HRP-C than in HRP-A2 (Yamasaki *et al.*, 1978; Dunford & Araiso, 1979). There are two histidine residues on the distal side of HRP-C, His40 and His42. His42 is presumed to coordinate to the iron. The propionic CO_2^- of the heme periphery or the side-chain CO_2^- of Asp43 may be important for formation of the first reaction intermediate (compound I) with H_2O_2 (Dunford & Araiso, 1979). These groups may stabilize the imidazolium ion in HRP-C.

In our earlier work (Austin *et al.*, 1975: Alben *et al.*, 1982; Alberding *et al.*, 1978; Doster *et al.*, 1982; Dlott *et al.*, 1983; Ansari *et al.*, 1986) we investigated recombination of O_2 and CO with myoglobin and other single-chain heme proteins by laser flash photolysis and i.r. spectroscopy over a wide range of temperature and time. We found that the following kinetic scheme described all experimental features in Mb:

$$A \overset{h\nu}{\rightleftharpoons} B \leftrightarrow M \leftrightarrow S + L. \qquad (S1)$$

A laser flash initiates photodissociation of the ligand L from the bound state A into the heme pocket B. The ligand can either recombine directly or move from B into the protein matrix M. Recombination $M \rightarrow B \rightarrow A$ or escape into the solvent is then possible. The protein state without ligand is denoted by S. Consequently one observes three processes: the internal process $I(B \rightarrow A)$, the matrix process $M(M \rightarrow B \rightarrow A)$, and the solvent process $S(S+L \rightarrow M \rightarrow B \rightarrow A)$. The rates and amplitudes of the three processes depend on temperature. Experiments over a wide range of temperatures allow the investigation of the individual steps of the reaction sequence. Below about 180 K, only process I is seen. It is non-exponential in time, suggesting that each protein can assume a large number of conformational substates (Austin *et al.*, 1975; Frauenfelder *et al.*, 1979).

The scheme (S1) leads to the following simple expressions for the association rate coefficient λ_S (Doster *et al.*, 1982; Young, 1984):

$$\lambda_S = \bar{k}_{BA} N_S P_B, \qquad (1)$$

where $\bar{k}_{BA}$ is the rate coefficient for step $B \rightarrow A$ averaged over all conformational substates; N_S is the fraction of recombination to initiate from the solvent; P_B is the "pocket occupation factor", i.e. the coefficient of the equilibrium $B \leftrightarrow S + L$ in the limit $k_{BA} \rightarrow 0$.

The reaction of CO with ferroperoxidase is more complex than with myoglobin. Our results imply a scheme with two bound states, A_1 and A_2 and consequently two pathways:

$$\begin{array}{l} \text{pathway (1): } A_1 \overset{I}{\leftrightarrow} B_1 \leftrightarrow (M) \leftrightarrow S+L \\ \qquad\qquad\qquad\qquad\quad B_2^* \overset{I^*}{\leftrightarrow} (M) \leftrightarrow \\ \text{pathway (2): } A_2 \overset{I}{\leftrightarrow} B_2 \end{array} \qquad (S2)$$

In this scheme we have introduced the matrix M in analogy to the scheme S1 that we found to be valid in Mb. We have, however, no direct evidence for the existence of M in HRP and consequently place it in parentheses. The absence of an observable matrix process is most likely due to the slowness of the transition $S+L \rightarrow B$. Under our experimental conditions, S and M are in dynamic equilibrium and cannot be distinguished.

i.r. spectroscopy implies that the states A_1 and A_2 correspond to two different carbonyl isomers. No internal exchange between pathways 1 and 2 is observed. The rebinding processes $B_1 \rightarrow A_1$ and $B_2 \rightarrow A_2$ have similar non-exponential kinetics and can be distinguished only at low temperatures. These two transitions are analogous to the well-studied process I in Mb. Pathway 2 has an additional state B_2^* with an optical spectrum different from deoxy HRP. B_2^* gives rise to a rebinding process I* that is fast (ns) even at the lowest temperatures and is exponential in time. A similar exponential rebinding process has been observed in carboxymethylated cytochrome *c* (cm-cyt *c*) (Alberding *et al.*, 1978). While the full scheme S2 is necessary for the description of CO binding to HRP at low temperatures, the simpler scheme S1 without M gives a sufficiently good approximation at physiological temperatures.

2. Materials and Methods

(a) *Sample preparation*

HRP prepared from horseradish and HRP type II from Sigma were used after further purification. The isoenzymes A2 and C were prepared by DAE and CM-cellulose column chromatography according to the method of Shannon *et al.* (1966). HRP-C ($Rz = 3·2$) had a typical activity of 300 units measured by the number of mg purpurogallin made in 20 s from pyrogallol at pH 6·0 and 20 °C. The activity of HRP-A2 ($Rz = 3·8$) was 100 units. Crude material (HRP type II, Sigma), which contains mainly HRP-C, was used also in some control experiments. The purity of the isozymes was checked by

gel electrophoresis. The results reported in this paper were not sensitive to slight differences in preparation. Even the crude material HRP type II had the same kinetic behavior as the purified isoenzyme HRP-C.

Ferroperoxidase was prepared in 0·1 M-phosphate buffer by anaerobic addition of a 10-fold molar excess of dithionite. Cryogenic samples contained 70% (v/v) glycerol. The protein concentration was about 50 μM for optical studies and 3 to 8 mM for i.r. experiments. The samples were equilibrated under 1 atm CO at room temperature (1 atm = 101,325 Pa).

(b) *Laser flash photolysis*

The laser flash photolysis system has been described earlier (Doster *et al.*, 1982). The photolyzing flash (25 ns, 300 mJ at 530 nm) was produced by a frequency-doubled neodymium-glass laser. Recombination after photolysis was monitored continuously from 100 ns, to 100 s by a Tektronix R7912 transient digitizer and a recorder with a logarithmic base. The monitoring light was produced by a tungsten source, filtered with interference filters, passed through the sample, and measured by a photomultiplier tube. The interference filters had a full width at half absorbance of 5 nm. Various filters were used with peak transmissions from 400 to 440 nm. The absorbance change could be measured to ±0·002 O.D. unit from milliseconds to 100 s. Slightly more error is present in the shorter time data because of photon fluctuations. The error at the shortest times is less than ±0·01 O.D. unit. A stabilized power supply is used for the monitor lamp, ensuring intensity drifts of less than 0·1% over the course of the experiment. A typical noise level is 0·002 O.D. unit.

The laser energy absorbed by the sample was adjusted to keep laser heating of the sample below 1·0 K at the lowest temperatures and less above. Hot spots can be excluded since the first data were taken 100 ns after the laser flash. At this time the heat is distributed uniformly over the sample. The conclusion follows from the heat conduction equation using the thermal conductivity and specific heat of glycerol and assuming a uniform distribution of absorption centers (proteins) in the sample.

(c) *Infrared spectroscopy*

The i.r. difference spectra between bound and photolyzed CO were taken with a Nicolet SC 7000 Fourier-transform i.r. spectrometer. The sample was placed between CaF_2 windows separated by a Teflon spacer whose thickness varied between 10 and 50 μm. It was mounted on a closed-cycle helium refrigerator equipped with CaF_2 windows (Lake Shore Cryotronics). The sample transmittance from 1000 cm^{-1} to 4000 cm^{-1} was measured with a resolution of 2 cm^{-1} with an InSb and a HgCdTe detector. The infrared difference spectrum was obtained as follows. The sample was cooled from 300 K to the target temperature in the dark and "dark" interferograms, taken over a period of 15 min. After illuminating the sample with a tungsten light source for 20 min, the "light" i.r. transmittance spectrum was measured. The reported spectrum is the absorbance difference spectrum $\Delta A(\nu)$, calculated at each wavenumber ν using the Beer–Lambert law:

$$\Delta A(\nu) \equiv A_D(\nu) - A_L(\nu) = \log I_L(\nu) - \log I_D(\nu),$$

where I_D and I_L are the transmittances measured in the dark and after illumination, respectively. We call these difference spectra "dark−light".

3. Results

(a) *Low-temperature experiments*

(i) *Step B → A (process 1)*

In Figure 1, we plot for HRP-C–CO the logarithm of the change in absorbance at 440 nm *versus* log time after photodissociation. Two different

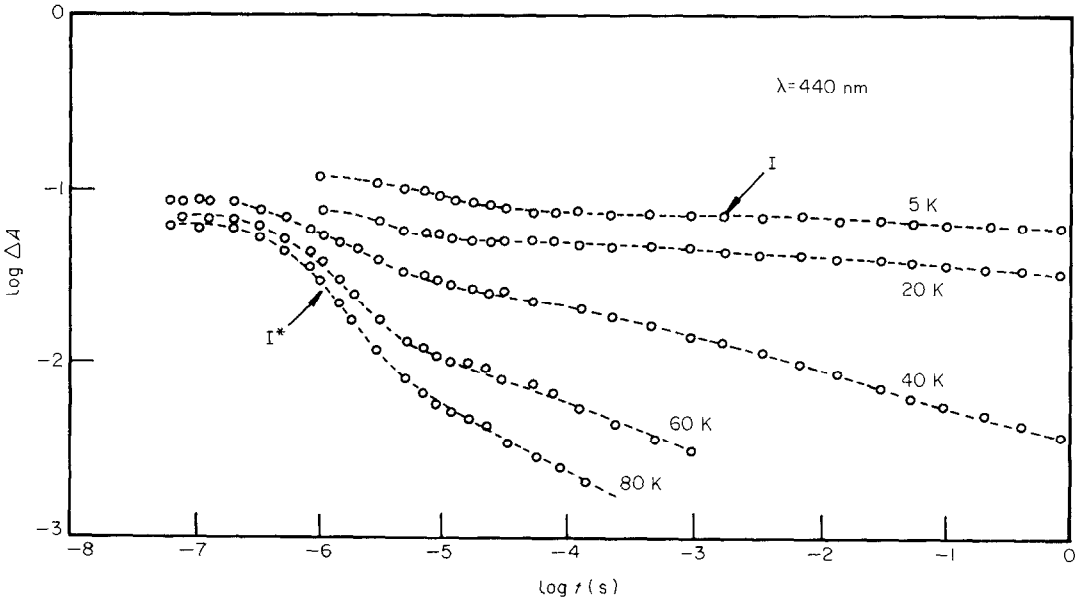

Figure 1. Rebinding of CO to HRP-C after photodissociation. The change in absorbance, ΔA, is plotted as log ΔA *versus* log t, where t is the time after the laser flash. Solvent: 70% glycerol/30% water (v/v) (pH 6·4). Monitoring wavelength 440 nm. The temperatures are labeled. The data points were block averaged to 3 points per decade and connected by straight lines.

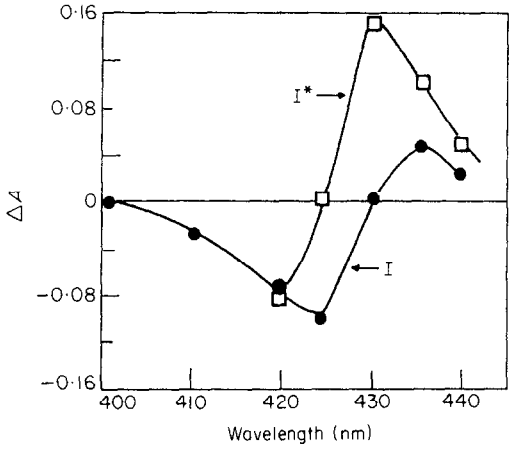

Figure 2. Soret spectral changes of processes I* (□) and I (●) at 40 K for HRP-C–CO (pH 6·4). The interference filters for the monitoring light have a full width at half-maximum of 5 nm.

recombination processes, I* and I, are observed. I* is fast and exponential in time, while I is slower and approximately follows a power law in time. The non-exponential kinetics of process I are attributed to a distribution of frozen conformational substates (Austin *et al.*, 1975). The exponential process I*, step $B_2^* \rightarrow A_2$ in S2, is a feature not seen in Mb. Figure 2 shows the Soret absorbance difference spectrum of HRP-C–CO and the kinetic intermediates B_1, B_2 and B_2^*. These spectra are measured 100 nanoseconds after photolysis for I* and ten microseconds after photolysis for I. B_1 and B_2 both show the deoxy spectrum and cannot be distinguished in the Soret region. The spectrum of B_2^*, however, is intermediate between deoxy and carboxy HRP. At 424 and 430 nm the absorbance change is small for process I* and I, respectively (Figs 3 and 5). Each process can be studied exclusively by selection of the proper wavelength without the need of kinetic decomposition. HRP-A2 also shows the processes I and I*, but displays an additional, very slow, low-intensity process at low temperatures. Repeated photolysis does not pump the system into this state. We do not include the very slow process in our discussion.

Process I can be analyzed using a distribution of activation enthalpies, $g(H_{BA})$ (Austin *et al.*, 1975; Young & Bowne, 1984). Such an analysis is straightforward for Mb and similar systems where only process I is observed. In HRP, the presence of I* complicates the analysis because the $\Delta A(t)$ curves are superpositions of processes I and I*. We cannot determine the relative number of proteins participating in the two processes, because the extinction coefficient of B_2^* is unknown. To analyze the data, we make the following simplifying assumptions:

(1) The spectra of states B_1 and B_2 are identical.

(2) The spectra of all states are time independent, and temperature independent over the range 2 to 180 K.

(3) States B_1 and B_2 both rebind with the same time course. With these assumptions, $N(t)$, the fraction of enzymes photolyzed at time t, is given by:

$$N(t) = f_I N_I(t) + f_{I^*} N_{I^*}(t),$$

where f_I (f_{I^*}) is the fraction of enzymes recombining *via* process I (I*). The function $N_I(t)$ has the value 1 at time zero, and decays with the same time course as the populations in states B_1 and B_2. Similarly, $N_{I^*}(0) = 1$ and $N_{I^*}(t)$ is proportional to the population in state B_2^* at time t. Using the $\Delta A(t)$ measured at 424 nm, where the absorbance of state B_2^* is negligible, $N_I(t)$ may be calculated from $N_I(t) = \Delta A(0)$, where $\Delta A(0)$ is independent of time

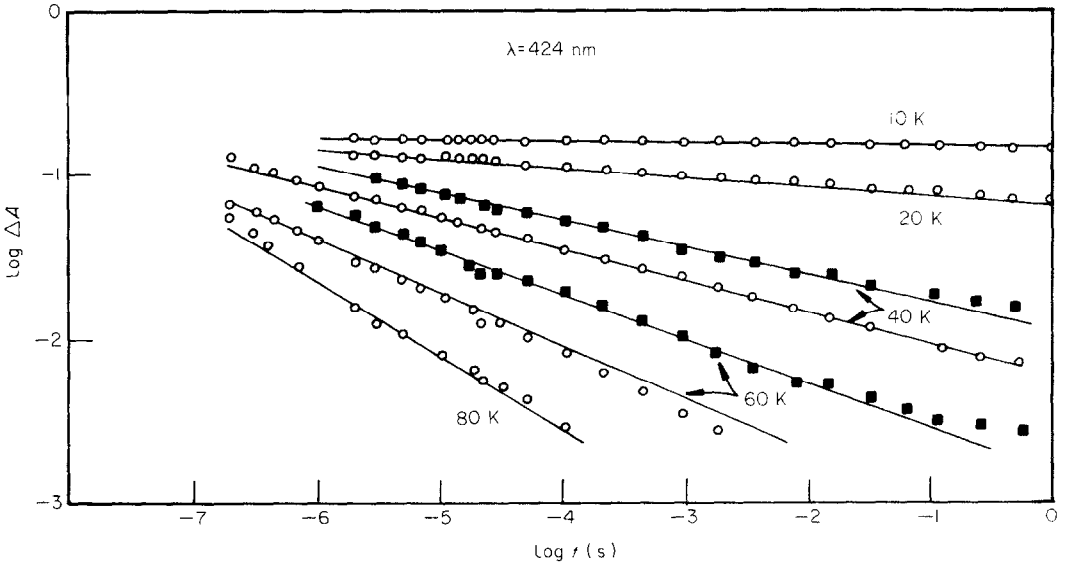

Figure 3. Rebinding of CO to HRP-A2 at $\lambda = 424$ nm (○) pH 8·3, (●) pH 5·8. A few representative data points are shown. The continuous lines represent fits according to the distribution $g(H_{BA})$ shown in Fig. 4. Only process I is observed at this monitor wavelength.

and temperature and is measured at 5 K and one microsecond. Similarly, $N_{I^*}(t)$ may be calculated from $\Delta A(t)$ at 430 nm, where the absorption of states B_1 and B_2 is negligible. With assumptions (1) to (3), $N_I(t)$ can now be expanded:

$$N_I(t) = \int_0^\infty dH_{BA} g(H_{BA}) e^{-k_{BA}t}. \quad (2)$$

If we assume further that the rate coefficient k_{BA} satisfies the Arrhenius relation, $k_{BA} = A_{BA} \exp\{-H_{BA}/RT\}$, we can use a numerical inversion of equation (2) to obtain $g(H_{BA})$. Inversion techniques have been discussed in various papers (Austin *et al.*, 1975; Provencher & Dovi, 1979; Doster *et al.*, 1982; Young & Bowne, 1984). The various techniques yield distributions $g(H_{BA})$ and values of A_{BA} that differ only insignificantly from each other and fit the measured $N(t)$ curves over a wide temperature range very well. Typically, the value of the peak of the enthalpy distribution, H_{BA}^{peak}, is determined to within less than1 kJ/mol and A_{BA} to within a factor of 2. The inversion results in the temperature-independent probability distribution shown in Figure 4, with parameters given in Table 1. Within the accuracy of our data, both isozymes HRP-C and HRP-A2 have the same distributions and pre-exponential.

In the analysis leading to Figure 4 and Table 1, we have assumed that all proteins possess the same pre-exponential factor, A_{BA}. If we distribute A_{BA}, but assume the same value of H_{BA} from all proteins, we cannot fit the data.

Process I of HRP-A2–CO was measured at pH 5 and pH 8·3 (Fig. 3). Recombination is slower at the lower pH. The effect of pH can be explained either by a shift of the enthalpy distribution by 1 kJ/mol or by a change of the pre-exponential factor by a factor of 2. We will show later that the pH effect at high temperatures favors the second explanation.

(ii) *Step $B_2^* \rightarrow A_2$ (process I*)*

Both isoenzymes show a fast exponential process I*. The rates k^* are the same within experimental uncertainty and are independent of pH. Process I* is faster than I below about 60 K and slower than most components of I above 60 K (Figs 3 and 5). The temperature dependence of k^*, shown in Figure 6, is rather unusual. Below 5 K, k^* is temperature independent. Between 5 and about 100 K, k^* increases weakly, less than linearly in T. Above about 100 K, k^* increases rapidly with T. The behavior above 100 K can be fit equally well by an Arrhenius law, with $A_{BA}^* = 5 \times 10^9\ s^{-1}$, $H_{BA}^* = 10{\cdot}5$ kJ/mol, or with a power law, $k^* \propto T^{9\pm1}$. The temperature dependence of k^* suggests that quantum mechanical tunneling dominates up to at least 100 K.

Table 1

*Parameters characterizing processes I and I**

System	pH	A_{BA} (s^{-1})	H_{BA}^{peak} (kJ/mol)	A_{BA}^* (s^{-1})	H_{BA}^* (kJ/mol)
HRP-A2	5	1×10^9	2·5	5×10^9	10·5
	8·3	2×10^9	2·5	5×10^9	10·5
HRP-C	6·4	1×10^9	2·5	5×10^9	10·5

The error in the pre-exponential is a factor of 2; the enthalpy error is less than 1 kJ/mol. Solvent: 70% (v/v) glycerol.

(iii) *Multiple flash experiments*

In a multiple flash experiment, a series of repetitive photolyzing flashes is applied to the sample, with the time between successive flashes chosen so that only a fraction of the HRP molecules have rebound a CO (Austin *et al.*, 1975; Frauenfelder, 1983). As demonstrated in Figure 3, process I has components slower than 100 seconds below 40 K. If the distribution of rates is caused by multiple states of the photolyzed ligand in each protein, it should be possible to pump all ligands into long-lived states by repetitive flashes 100 seconds apart. We observe, however, that only the high-energy tail of the enthalpy distribution is cut off, indicating a heterogeneous sample of proteins with non-interconvertible conformational substates.

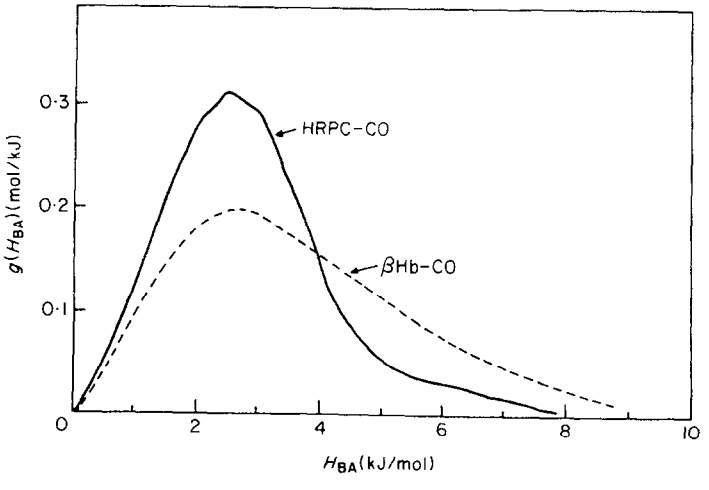

Figure 4. Enthalpy distribution of HRP–CO (——) and βHb–CO (– – –).

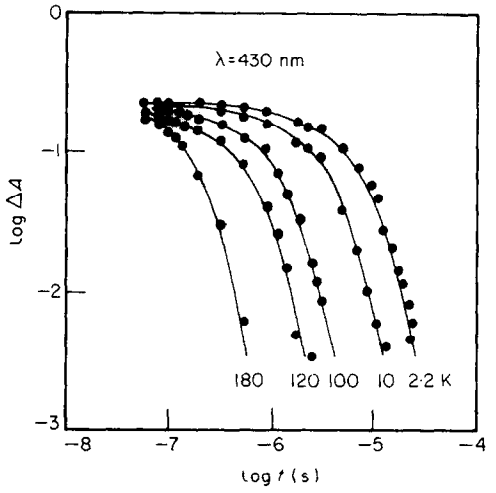

Figure 5. Data points: changes of absorbance *versus* log time of HRP-C–CO at 430 nm monitor wavelength (pH 6·4). Only process I* is observed at this wavelength. The continuous lines show fits to a single exponential.

The amplitude of the exponential process I* decreases below 40 K after multiple flashes, and I increases. We conclude that the I* intermediate B_2^* is connected with a deoxy state B_2 that rebinds *via* process I, as indicated in scheme S2. Moreover, the multiple flash experiment proves that I and I* occur in the same protein molecule and rules out sample heterogeneity.

(iv) *Relation between I and I*: infrared experiments*

The observation that two processes with different optical and kinetic properties take place at low temperatures raises two questions. Do the two processes I and I* occur in the same or in different molecules? If they occur in the same molecule, are they in sequence or in parallel?

The first explanation for the occurrence of I and I*, heterogeneity of the sample, can be excluded, since the purity of the isoenzymes was checked by gel electrophoresis. Furthermore process I* occurs in both isoenzymes and I* can be pumped into I even at low temperatures. We consequently conclude that I and I* occur in the same molecule, as shown in scheme S2.

I and I* in the same protein can be either sequential or parallel. The sequential models can be excluded, because process I* is faster than I at 40 K but slower at 100 K (Figs 3 and 5). In a sequential scheme:

$$A \xleftarrow{I^*} B^* \xleftarrow{I} B,$$

I* should always be faster. We consequently assume parallel pathways as in S2.

The existence of two different pathways, 1 and 2, as shown in scheme S2 follows from i.r. data. The i.r. spectra of HRP-C–CO and HRP-A2–CO have two CO-stretching bands and this implies the existence of two different bound states, A_1 and A_2

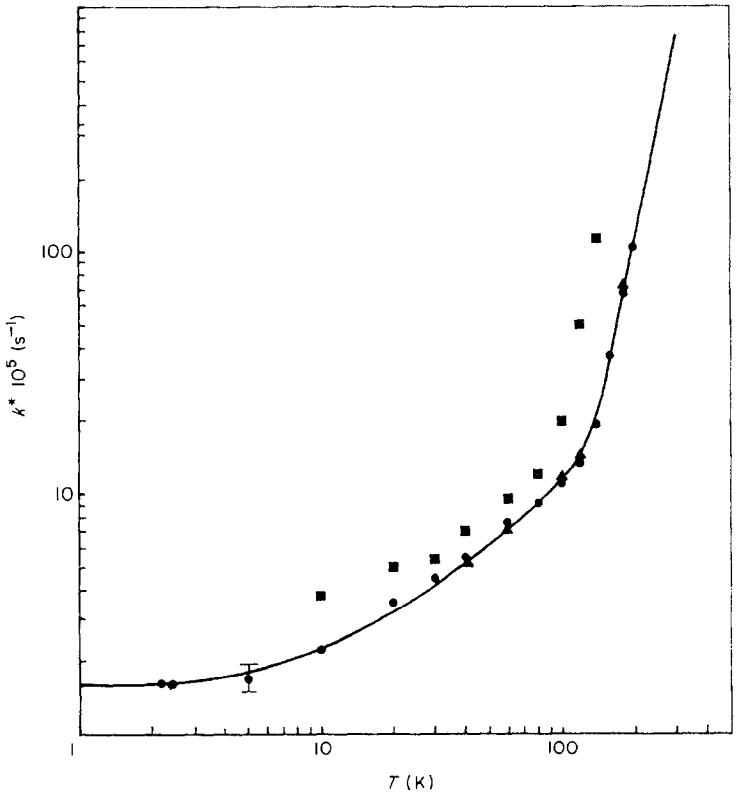

Figure 6. Rate coefficient k^* of $B_2^* \rightarrow A_2$ for HRP-C (○), HRP-A2 (▲) and cm-cyt *c* (■). The HRP data were taken at $\lambda = 430$ nm. The line is a fit to a phonon-assisted tunneling model to the HRP data: $k^* = a + b \coth(c/2kT) + A^*_{BA} \exp(-H^*_{BA}/RT)$, $a = 1{\cdot}1 \times 10^5\ s^{-1}$, $b = 3{\cdot}6 \times 10^4\ s^{-1}$, $c = 3{\cdot}5$ K. The cm-cyt *c* data are shown for comparison.

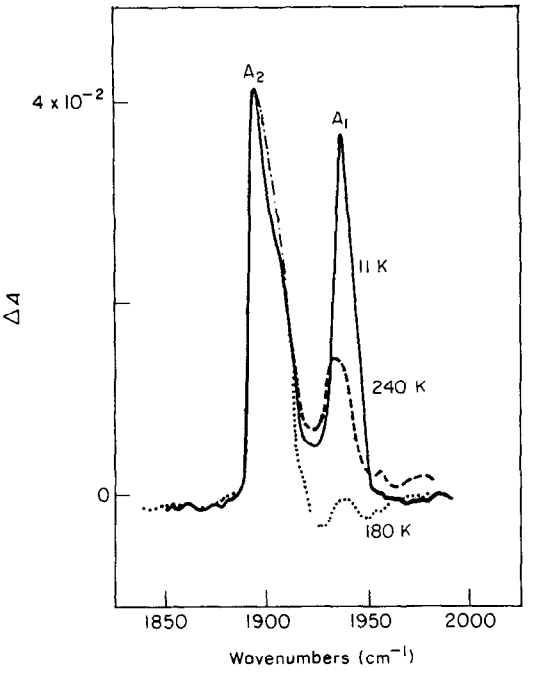

Figure 7. Dark−light absorption difference spectra of HRP-C–CO (pH 6) at 11, 180 and 240 K. At 11 K, the sample can be completely photolyzed and both bound states A_1 and A_2 can be seen. At 180 K only state A_2 is visible because the proteins that form band A_1 rebind quickly *via* process I. Upon photolysis at 240 K some proteins from band A_1 lose their CO to the solvent, so band A_1 is visible again. The calculation of ΔA is described in the text. Peaks above the baseline correspond to spectral features of the dark or bound state while peaks below the baseline are features of the photolyzed state.

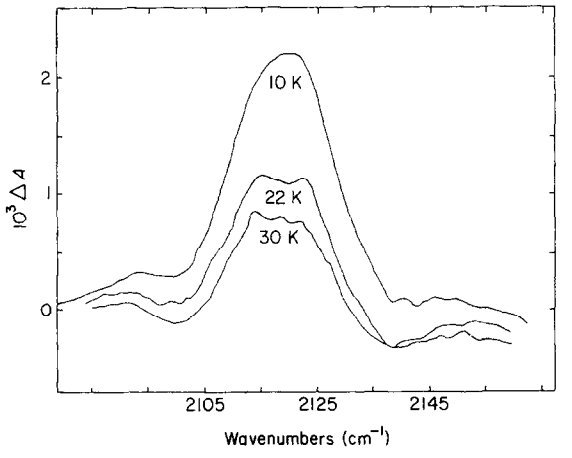

Figure 8. B state dark−light absorption difference spectra of HRP-C–CO (pH 6) at 10, 22 and 30 K. After photolysis at 10 K the B state absorption can be seen as a single broad peak. The sample was heated in the dark to 22 K and 30 K, where spectra were measured without further dissociation. The peak shape is nearly temperature independent. The overall decrease in peak area is due to partial recombination of CO during the experiment.

(Alben & Bare, 1973). HRP-C has a pH-independent absorption at 1933 cm^{-1} (A_1) and a second band at 1905 cm^{-1} (A_2) which shifts to 1929 cm^{-1} at pH > 9 (Barlow *et al.*, 1976). Our i.r. difference spectra (dark−light) between CO-bound and photolyzed HRP-C at various temperatures, given in Figure 7, show the two bands. At 11 K, the peak wavenumbers are at 1935 cm^{-1} for A_1 and 1895 cm^{-1} for A_2.

The difference bands at 1895 cm^{-1} and 1935 cm^{-1} decay with the same time dependence if the bound sample is photodissociated at 11 K and then heated. The two processes I, $B_1 \rightarrow A_1$ and $B_2 \rightarrow A_2$, consequently have the same non-exponential kinetics at low temperatures. However, the behavior of the states A_1 and A_2 under constant illumination at low temperatures is different: A_2 appears to dissociate more slowly than A_1. This observation is explained if the fast transition I* occurs in pathway 2 as shown in scheme S2. Even though the intrinsic quantum yields of A_1 and A_2 may be the same, the HRP molecules that reach state B_2 rebind quickly even at very low temperatures and the effective quantum yield is reduced.

The dark−light difference spectra provide additional information at 180 K and above. As Figure 7 shows, the A_1 peak is much smaller than the A_2 peak at 180 K: B_1 appears to rebind much faster than $B_2 + B_2^*$. This observation can again be explained if I* is assigned to pathway 2. At 180 K, I* is much slower than I. Thus under constant illumination A_2 is more efficiently pumped into the matrix M *via* B_2^* than *via* A_1, which has only one path. Once CO is in the matrix or the solvent, return to B is very slow. Consequently pathway 2 appears to be much slower than pathway 1 at 180 and 240 K.

The assignment of I* to pathway 2 is unambiguously verified by a "pumping" experiment. HRP–CO is photolyzed at 180 K and then cooled rapidly to 40 K. As Figure 7 shows, A_1 rebinds quickly at 180 K, but A_2 does not. The cooled sample thus consists of a mixture, with most of the states A_1 occupied and most of the states A_2 vacant. Photodissociation of this mixture predominantly sees pathway 1. The experiment shows a decrease of the amplitude of process I* by a factor of more than 4, while the amplitude of process I decreases by only about 50%. I* consequently must be connected to A_2. We conclude that HRP has two CO isomers that give rise to different recombination processes. In isomer I, the bound state A_1 has a CO stretching frequency of 1935 cm^{-1} at 14 K and photolyzes into a single unbound state B_1. In isomer 2, the bound state A_2 has a CO stretching frequency of 1895 cm^{-1} at 14 K, and photolyzes into two unbound states B_2 and B_2^*. Therefore, isomer 2 contributes to process I and is solely responsible for process I*.

Figure 8 shows the i.r. absorption spectra of photolyzed HRP-C–CO. One broad temperature-independent peak is seen, with center frequency

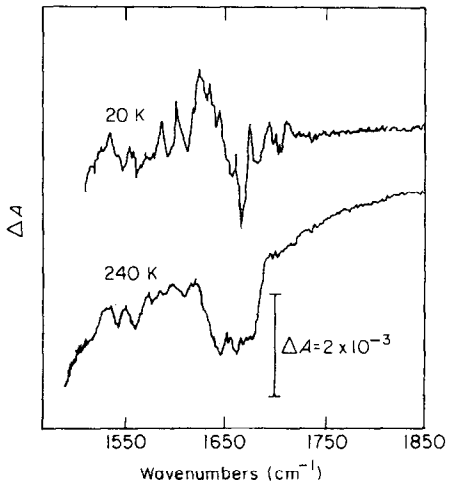

Figure 9. Dark−light difference spectra of HRP-C–CO (pH 6) at 20 K and 240 K in the amide I/II region. The difference spectrum at 20 K indicates that a band near 1650 cm^{-1} has shifted to lower wavenumbers upon photolysis. At 240 K, there is a decrease in total absorption near 1650 cm^{-1} upon photolysis.

2118 cm^{-1} and width $\Delta\nu_{1/2} = 20$ cm^{-1}. This spectrum implies that there are several photolyzed states in HRP-C–CO that do not thermally interconvert. In contrast, photolyzed MbCO shows two narrow ($\Delta\nu_{1/2} = 5$ cm^{-1}) bands at 2130 cm^{-1} and 2119 cm^{-1} (Alben *et al.*, 1982). These bands are strongly temperature-dependent from 4 K to 20 K. The shift of 25 cm^{-1} relative to CO in the gas phase (2143 cm^{-1}) and the absence of rotational sidebands indicates libration of the CO molecule in the heme pocket of HRP.

(v) *Conformational changes*

In the subsection (d), above, we discussed dark−light i.r. spectra in the region of the CO stretch frequency, 1850 to 2150 cm^{-1}. We have taken similar spectra in the amide I/II region, 1550 to 1650 cm^{-1}. The sample in the liganded state is cooled to the desired temperature and the difference spectrum between the liganded (dark) and the photodissociated state (light) is recorded. Figure 9 shows the difference between spectra of HRP-C–CO and its photolyzed state at 20 and 240 K. At 20 K, Figure 9 shows a positive peak near 1630 and a negative peak near 1650 cm^{-1}, indicating that an absorption peak has shifted toward lower wavenumber after photodissociation. At 240 K the dark−light spectrum has a broad negative peak that indicates a decrease of the total absorption at 1650 cm^{-1}. We interpret these results as showing conformational changes after photodissociation (Ansari *et al.*, 1985). At 20 K, the protein relaxes partially toward the deoxy structure; at 240 K, relaxation has progressed further. The absorption changes accompanying these conformational changes are as large as the ones involved in the CO stretching peaks.

(b) *Kinetics at intermediate and high temperatures*

The kinetics of CO recombination from the solvent of HRP-C are shown in Figure 10. In the temperature range between 220 K and 330 K, only a single process S+L → A is found. The matrix process M → A, which is dominant at 240 K in Mb and related proteins, is not observable in HRP. The solvent process is a single exponential:

$$N(t) = N_S \exp\{-\lambda_S t\}. \quad (3)$$

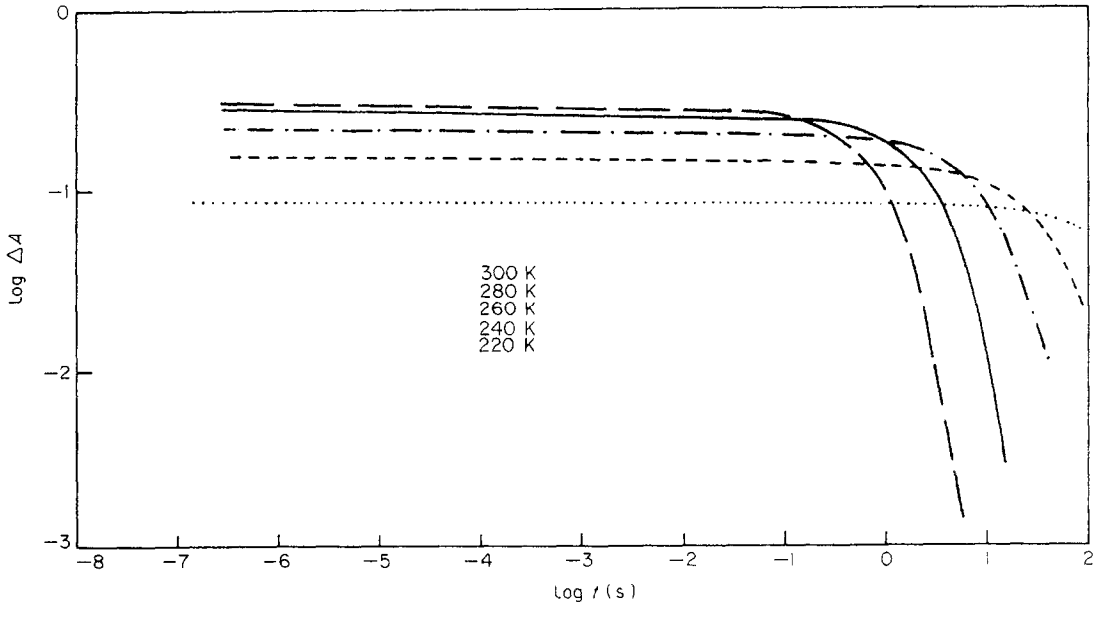

Figure 10. Binding of CO to HRP-C after photodissociation. Solvent: 70% glycerol/30% water (v/v) (pH 6·4). Observation wavelength 440 nm. Above about 200 K some CO molecules escape into the solvent. Rebinding from the solvent (process S) is exponential in time and slow. The decreased absorbance change at low temperatures is presumably caused by fast geminate recombination.

Here $N(t) = \Delta A(t)/\Delta A_{max}$, where ΔA_{max} is independent of time and temperature and represents the absorbance change of the sample if all the enzymes were in state S. We use the absorbance change at 300 K one millisecond after flashoff as our estimate of ΔA_{max}. As before, $N(t)$ is the fraction of enzymes with a bound CO. λ_S is proportional to the CO concentration in the solvent. The mono-exponential character of the solvent process suggests that S2 can be simplified above 200 K. In the low temperature section we have seen that geminate recombination of deoxy HRP and CO involves $B_1 \rightarrow A_1$, $B_2 \rightarrow A_2$. These processes can be monitored by the decays of the 1895 cm^{-1} and 1935 cm^{-1} CO bands. Both bands decay with approximately the same rate. We therefore assume a single internal process $B \rightarrow A$ for the analysis of process $S + L \rightarrow A$. We assume further that the rate $\bar{k}_{BA}$ above 200 K can be calculated as an average from the enthalpy distribution $g(H_{BA})$:

$$\bar{k}_{BA} = \int_0^\infty k_{BA}(H_{BA},T)g(H_{BA})\,dH_{BA}. \qquad (4)$$

Such an extrapolation procedure was shown to apply to β-chains of human hemoglobin (Ansari *et al.*, 1986). By neglecting the matrix process we arrive at the simple kinetic scheme S1′:

$$A \leftarrow B \leftrightarrow S + L \qquad (S1')$$

λ_S is given by equation (1), P_B and N_S can be written in terms of rate coefficients:

$$N_S = k_{BS}/(\bar{k}_{BA} + k_{BS}), \qquad (5)$$

$$P_B(c,T) = k_{SB}/k_{BS}, \qquad (6)$$

and $P_B(c,T)$ is proportional to the CO concentration, c, in the solvent.

With these relations, the evaluation of the data at intermediate and high temperatures is straightforward. For a given solvent, a fit of equation (3) to the data in the form of Figure 10 yields the parameters $N_S(T)$ and $\lambda_S(T)$. The low-temperature data and equation (4) give $\bar{k}_{BA}(T)$. Equations (1) and (5) together then determine $P_B(c,T)$, $k_{BS}(T)$ and $k_{SB}(T)$. Assuming Arrhenius relations for these three coefficients,

$$k_{BS} = A_{BS} \exp\{-H_{BS}/RT\},\ k_{SB} = A_{SB} \exp\{H_{SB}/RT\},$$

and:

$$P_B(c,T) = P_0(c) \exp\{-H_B/RT\}, \qquad (7)$$

permits the determination of the parameters $P_0(c)$, H_B, H_{BS}, A_{BS}, H_{SB} and A_{SB}. The parameters are listed in Table 2.

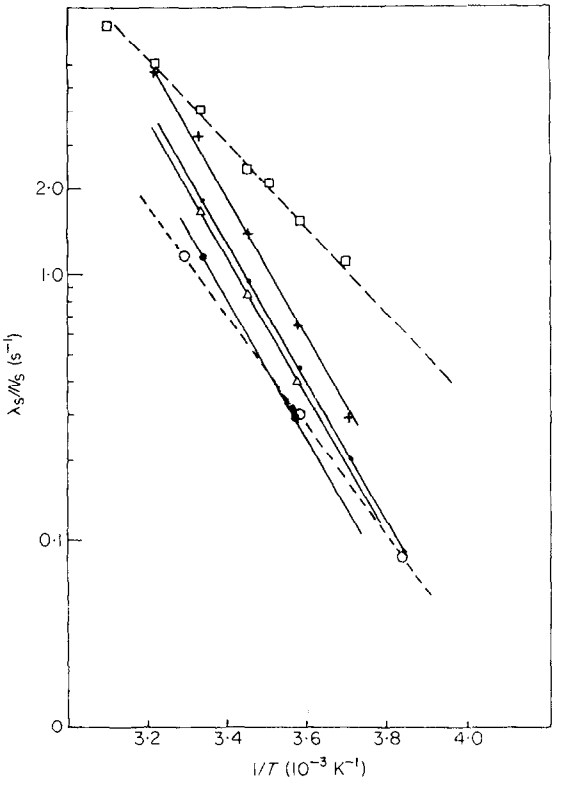

Figure 11. λ_S/N_S of HRP-C and HRP-A2 *versus* inverse temperature at various conditions: HRP-A2: (+) water, [pH 8·3, (△) water, pH 5·8, (●) 70% glycerol/30% water, pH 8·3, (◐) 70% glycerol/30% water. pH 5. HRP-C: (□) water, pH 6, (○) 70% glycerol/30% water, pH 6·4.

Figure 11 shows the influence of pH and solvent in $\lambda_S/N_S = \bar{k}_{BA}P_B(c,T)$. Consider first the influence of pH. The recombination rate is slower at low pH, consistent with a pH-independent activation enthalpy and a change in the pre-exponential factor A_{BA} by 1·8. The fact that the pH dependence of the step $B \rightarrow A$, measured at low temperatures (Fig. 3), agrees with the pH dependence of the overall binding coefficient λ_S, measured near 300 K, supports the sequential schemes S1 and S2.

Figure 11 also indicates that an increase in solvent viscosity decreases the association rate coefficient, λ_s, in agreement with the observation made with Mb (Beece *et al.*, 1980).

A remarkable result in Table 2, the small value of $P_B(c,T)$, is reflected in the high Gibbs energy of the

Table 2

Parameters characterizing the transitions $B \rightarrow S$ and $S \rightarrow B$

System	pH	k_{BA} (300 K) (s^{-1})	A_{BS} (s^{-1})	H_{BS} (kJ/mol)	A_{SB} (s^{-1})	H_{SB} (kJ/mol)	P_B (300 K)†	P_0	H_B (kJ/mol)
HRP-A2	5	$3{\cdot}7 \times 10^8$	$1{\cdot}5 \times 10^{11}$	14	7×10^{10}	61	1×10^{-8}	1	46
	8·3	$7{\cdot}4 \times 10^8$	$1{\cdot}5 \times 10^{11}$	14	7×10^{10}	61	1×10^{-8}	1	46
HRP-C	6·4	$3{\cdot}7 \times 10^8$	$2{\cdot}0 \times 10^{11}$	15	1×10^9	50	1×10^{-8}	0·003	31

† P_B refers to 1 atm CO and 300 K and to water as solvent.

pocket state B. We discuss this result in more detail later.

4. Discussion

In this section, we discuss the main results obtained with HRP. Of particular interest are similarities and differences between HRP and the oxygen storage and transport proteins Mb and Hb.

(a) *Kinetic scheme*

Ligand binding in Mb and in hemoglobin monomers is adequately described by the sequential scheme S1 (Austin *et al.*, 1975; Dlott *et al.*, 1983; Ansari *et al.*, 1986). The results obtained in the present paper indicate that the general features of the sequential scheme are valid also for HRP, but that characteristic differences exist.

(1) The binding step B → A is more complex in HRP than in Mb, owing to the formation of different carbonyl isomers in HRP. Evidence for these isomers comes from the CO stretching frequencies A_1 and A_2 in the bound state A, shown in Figure 6 and from resonance Raman spectroscopy (Evangelista-Kirkup *et al.*, 1986). The peak position at 1895 cm^{-1} for $^{12}C^{16}O$ in state A_2 is anomalously low. Moreover, the Soret difference spectrum of process I* is very different from that of process I, as shown in Figure 2. Therefore the state B_2^* is very different from states B_1 and B_2, and the state A_2 may also differ considerably from A_1. No internal conversion between states A_1 and A_2 or between B_1 and B_2 is observed. Barlow *et al.* (1976) suggest from their i.r. measurements at room temperature that HRP has (at least) two niches for CO. No internal pathway between these niches seems to exist. The ligand has to go to the solvent to change niches.

(2) The data provide no evidence for a matrix state M. This result is at first surprising because HRP (M_r 44,000) is much larger than Mb (M_r 18,000). We believe that M is obscured by the properties of state B, which will be discussed in subsection (e), below. The matrix process was also not seen in cm-cyt *c* and heme octapeptide, which show a process I* (Alberding *et al.*, 1978).

(b) *Process I*

The Soret spectrum of photolyzed CO–HRP at low temperatures is nearly identical with that of deoxy-HRP. The ligand in the pocket is therefore not close enough to influence the electronic properties of the heme. Recombination is non-exponential in time and can be analyzed using a temperature-independent distribution of activation enthalpies $g(H_{BA})$. Such a distribution of frozen conformational substates has been observed in all heme proteins that we have studied. The peak enthalpy of 2·5 kJ/mol is comparable with that of the β-chain of hemoglobin, but is considerably smaller than the H_{BA}^{peak} of myoglobin (10 kJ/mol).

The pre-exponential A_{BA} of 2×10^9 s^{-1} is close to that found for hemoglobin monomers and myoglobin. The small value of A_{BA} has been taken as evidence for a non-adiabatic reaction (Jortner & Ulstrup, 1979). The high spin–low spin transition ($S = 2 \rightarrow S = 0$) requires second-order spin orbit coupling and should control the reaction. The fact that A_{BA} is the same for O_2 and CO in many heme proteins casts doubt on this interpretation. Frauenfelder & Wolynes (1985) have discussed the problem in detail. They suggest that friction and steric effects can render a non-adiabatic transition adiabatic. In fact a value of A_{BA} close to the experimental one can be derived from the loss of translational entropy between state B, in which the ligand occupies a free volume of about 30 $Å^3$ (1 Å = 0·1 nm) in Mb (Doster *et al.*, 1982) and the transition state. The observation that process I can be fit by a sharp A_{BA} implies that the volume (entropy) distribution is narrow. As in hemoglobin monomers and Mb process I of HRP depends upon pH. However, while in Mb and β^A recombination is faster at low pH, the opposite is observed in HRP-A2. A parallel change of λ_S at high temperatures is observed in these proteins, supporting a sequential scheme. All of these proteins have a heme-linked distal protonation group that has been studied by a number of techniques (Teraoka & Kitagawa, 1981; Barlow *et al.*, 1976; Hayashi *et al.*, 1976; Doster *et al.*, 1982). The importance of this group will be discussed in the next section.

(c) *The nature of process I**

HRP, cm-cyt *c*, and heme octapeptide have a fast exponential process I*, which is not found in myoglobin and other oxygen-transport heme proteins. Its occurrence in connection with catalysis and electron transport may be relevant. I* might indicate properties of the heme group that are necessary for catalysis of peroxidation or electron transport. In the following, we list a number of properties that together can cause a fast exponential process.

First of all the spectrum of B_2^* resembles the carboxy spectrum, but is red-shifted by 6 nm. A red-shift in the Soret band indicates an increase in the Fe–N^ε (His) bonding interaction either by an Fe spin transition or steric factors (Perutz, 1979; Schmidt & Reed, 1981; Martin *et al.*, 1984). The CO in state B_2^* may still be close enough to prevent relaxation of the heme group. Such an effect can be expected if the motion of the ligand is sterically hindered by either close packing or a hydrogen bond. Such a hydrogen bond has been postulated for CO complexes of peroxidase but not for myoglobin (Teraoka & Kitagawa, 1981; Barlow *et al.*, 1976; Hayashi *et al.*, 1976; Campbell *et al.*, 1982). Central to our discussion is therefore a distally heme-linked protonation group and its pH dependence. Spectrophotometric titration and proton balance measurements indicate that the pK_a

value of this group in HRP-C is shifted from 7·25 to 8·25 upon combination with CO. The shift is much smaller in Mb, from 5·57 to 5·67 (Hayashi *et al.*, 1976). Hayashi *et al.* concluded that the shift of the pK_a in the case of peroxidase can be explained by the existence of a hydrogen bond between the sixth ligand and the distal base.

The Fe-proximal histidine stretching Raman line also exhibits a frequency shift of 8 cm^{-1} with pH in HRP but not in Mb (Teraoka & Kitagawa, 1981). The pK_a values were 7 and 5·5 for HRP-C and HRP-A2, respectively. These Raman data are not compatible with deprotonation of the proximal histidine at low pH. Instead, Teraoka & Kitagawa suggest that the distal histidine is deprotonated, causing a conformational change that exerts strain on the Fe-proximal histidine bond at high pH. This idea is supported by nuclear magnetic resonance (n.m.r.) experiments, which show that the proximal histidine is not deprotonated at high pH (LaMar *et al.*, 1982).

Additional information comes from the stretching frequency of CO bound to HRP. The data are summarized in Table 3. The two important bands, A_1 and A_2, are assigned to CO bound to the heme iron in two different geometries (Barlow *et al.*, 1976). The high frequency band A_1 (1938 cm^{-1} in A2 and 1933 cm^{-1} in C) is independent of pH. The frequencies are within the range found in other heme proteins. The band is assigned tentatively to a CO bound normally to the heme plane and not hydrogen bonded (Evangelista-Kirkup *et al.*, 1986). The low-frequency band A_2 shifts from 1933 cm^{-1} in HRP-A2 and 1929 cm^{-1} in HRP-C at high pH to 1906 and 1905 cm^{-1} at low pH with pK_a values of 6·7 (A2) and 8·8 (C) (Barlow *et al.*, 1976). This extremely low frequency band is tentatively assigned to a CO bound in a tilted geometry and forming a hydrogen bond with a protonated distal histidine residue (Evangelista-Kirkup *et al.*, 1986).

We find that the I* intermediate ($B_2^{\ddagger}$) arises from the 1895 cm^{-1} A_2 state by photolysis. The hydrogen bond and the proximity of a protonation group seem to restrict the motion of the ligand away from the iron. The strength of the hydrogen bond has little influence on the rate of process I*: k^* is independent of pH.

A protonation group seems to exist also in cm-cyt *c* (Brunori *et al.*, 1972), but i.r. Raman and n.m.r. data are not available for this enzyme. The most unexpected feature of process I* is its exponential dependence on time, while power-law kinetics are usually observed at low temperatures in heme proteins. Process I of Mb involves a motion of the iron into the heme plane in parallel with a spin transition. As a high-to-low-spin transition is caused by a change of symmetry, it was suggested that the I* intermediate in cm-cyt *c* has the heme iron still in plane, trapped in a singlet or triplet state (Alberding *et al.*, 1978). Therefore no change of symmetry occurs and process I* is not influenced by the distribution of conformational substates. A necessary condition for the iron to stay in plane and close to the ligand in the photolyzed state is the rigidity of the heme group and its environment. This idea is supported by several experiments. The iron–His stretching frequency of HRP (244 cm^{-1}) is substantially higher than in myoglobin and hemoglobin (220 cm^{-1}) (Teraoka & Kitagawa, 1981). It is interesting, however, that HRP and Mb exhibit only one Raman band but two i.r. CO stretching bands. Furthermore n.m.r. data show that the proximal histidine of reduced HRP is protonated (LaMar *et al.*, 1982). The exchange half-life of the N_1H proton is approximately 13 minutes at 35°C and pH 6·2. The corresponding exchange rate in myoglobin is of the order of tens of milliseconds. Since large exchange rates with bulk water of internal labile protons indicate flexibility, it can be concluded that HRP is much tighter and less flexible than myoglobin. The rigidity of the heme group on its proximal side and the restricted mobility of the ligand by hydrogen bonding on the distal side may be necessary conditions for the occurrence of process I*.

(d) *Process I*: molecular tunneling*

Figure 6 shows the rate coefficients k^* for process I* in HRP-C–CO, HRP-A2–CO and cm-cyt *c*–CO.

Table 3

Infrared stretching frequencies of $^{12}C^{16}O$ bound to heme iron for various proteins

Protein	Solvent	Temperature (K)	pH	A_1 (cm^{-1})	A_2' (cm^{-1})	A_2 (cm^{-1})	Comments
HRP-C†	75% glyc.	10–180	7	1935	—	1895	A_1 and A_2 do not interconnect at low temperature
HRP-C‡	Water	293	9	1933	1929		A_2' titrates into
			5	1933		1906	A_2 with $pK_a = 8·8$
HRP-A2‡	Water	293	7	1938	1925		A_2' titrates into
				1938		1905	A_2 with $pK_a = 6·7$
Mb§	75% glyc.	5·5–200	7	1944·8	—	1927	

glyc., glycerol.
† This work.
‡ Barlow *et al.* (1976).
§ Alben *et al.* (1982).

In all three proteins, I* is exponential in time. Within experimental errors the isoenzymes HRP-A2 and HRP-C have the identical time dependence; k^* in cm-cyt c has the same form, but is somewhat faster. Between 2 and 200 K, the HRP data can be fit well by an expression of the form:

$$k^*(T) = a + b \coth(c/T) + A^*_{BA} \exp\{-H^*_{BA}/RT\}, \quad (8)$$

with $a = 1{\cdot}1 \times 10^5\ s^{-1}$, $b = 3{\cdot}6 \times 10^4\ s^{-1}$, $c = 3{\cdot}5$ K, $A^*_{BA} = 5 \times 10^9\ s^{-1}$, $H^*_{BA} = 10{\cdot}5$ kJ/mol. An equally good fit is obtained by replacing the last term in equation (8) by dT^m, with $d = 2 \times 10^{-14}\ s^{-1}\ K^{-9}$, $m = 9$ (Fig. 6).

The fact that the time and temperature dependences are so similar in HRP-A2, HRP-C and cm-cyt c suggests a common mechanism. Four prominent aspects must be explained: the similarity of process I* in three proteins and in heme octapeptide, the red-shifted Soret spectrum of state B^*_2, the exponential time dependence of k^*, and the remarkable temperature dependence of k^*. We have already discussed some of the relevant data in subsection (c), above, and summarize here the main points.

The similarity of I* in the different proteins and the model compound suggests that the heme group dominates the reaction and the globin is only weakly involved. The simplest explanation then is the one already introduced: I* corresponds to rebinding of the CO before the Fe atom has moved out of the mean heme plane into the deoxy position. This model may also explain the exponential time dependence: with the Fe in the heme plane and the CO close by, there may be very few conformational substates available so that the binding is governed by a unique barrier.

The temperature independence of k^* below 5 K and the less than linear temperature dependence up to 100 K suggests molecular tunneling (Goldanskii, 1979; Hänggi *et al.*, 1985). Nuclear tunneling is normally observable only at very low temperatures owing to the exponential mass dependence of the tunneling rate, but has been seen for process I in β^A and Mb up to 40 K (Alberding *et al.*, 1976; Frauenfelder, 1979; Alben *et al.*, 1980). Indeed the first two terms in equation (8) can be interpreted as describing the temperature-independent low-temperature limit of tunneling and the single-phonon-assisted regime. Difficulties arise when the third term is considered. The obvious explanation for the steep increase in k^* above about 100 K is to assume a classical Arrhenius motion over a barrier of height 10·5 kJ/mol. Consider now the well-known expression for the rate coefficient k_t for tunneling through a parabolic barrier (Landau & Lifshitz, 1958):

$$k_t = A_t \exp\{-\pi(2MH)^{1/2}d/2\hbar\}. \quad (9)$$

Here H is the barrier height, d the barrier width, and M the mass of the tunneling system. Using a tunneling pre-exponential factor of $A_t = 10^9\ s^{-1}$, a mass corresponding to the CO molecule, and a tunneling rate coefficient $k_t = 10^5\ s^{-1}$ (Fig. 6) yields a barrier width of $d \approx 20$ pm. Such a narrow barrier is not inconsistent with the Soret spectrum of B*, which is intermediate between carboxy and deoxy HRP. The ligand in B* may be close enough to the heme to influence its electronic properties. Moreover, the estimate of d is based on a simple tunneling model, assuming a point particle. A realistic model may yield a larger d. A problem is caused by the large barrier height $B^*_2 \rightarrow A_2$, however, and we have no easy explanation for the value of about 10 kJ/mol implied by the assumed Arrhenius relation.

In a second explanation of the steep increase we can assume that it is described by a power law, $k^* \propto T^9$, and that the increase is caused by multi-phonon-assisted tunneling. The classical Arrhenius process than would set in at even higher temperature and thus demand an even higher barrier than in the case discussed above. So an even higher barrier would have to be explained.

A third explanation for the change of slope in k^* at about 100 K involves conformational relaxation. Conformational relaxation can lead to an increased barrier height and decreased rate (Agmon & Hopfield, 1983). Some relaxation may, however, lead to a faster transition.

The unusual properties of process I* pose a challenge both for further experimental studies and for theoretical investigations.

(e) *Recombination at high temperatures*

The association rate coefficient λ_S is connected to the coefficient $\bar{k}_{BA}$ by equation (1). Fast rebinding at low temperatures, therefore, will usually imply fast binding at room temperature. Such a correlation has been found for many heme proteins (Stetzkowski *et al.*, 1985) and it implies that the coefficients P_B in different proteins have the same order of magnitude, about 10^{-4} to 10^{-5} at 1 atm CO pressure above the sample. HRP is an exception. Low temperature binding is very fast, as shown in Figure 1 and described by the parameters in Table 1. In contrast, association at room temperature is extremely slow (Fig. 10). These two observations together lead to the conclusion that P_B, the partition coefficient of CO in the heme pocket, is about 10^{-8}, smaller by a factor 10^4 than for Mb. P_B also shows a strong temperature dependence. The data in Figure 11 together with equations (4) and (7) yield the values of P_0 and H_B listed in Table 2. H_B is the enthalpy difference between CO in the solvent and in the heme pocket. For HRP-A2, $H_B = 46$ kJ/mol compared to about 2 kJ/mol for Mb (Fig. 12). Such a large value cannot be explained by a rigid protein. We have to assume that binding includes a conformational transition and a large increase of structural Gibbs energy. This idea is supported by a large change of the amide I band upon photolysis at 240 K, where the ligand moves into the solvent (Fig. 9). The width of the dip in the difference spectrum is about

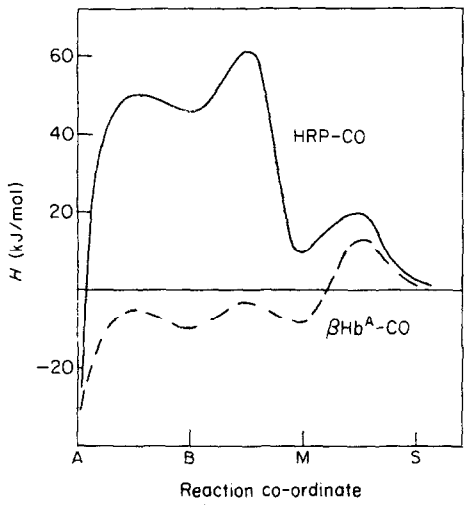

Figure 12. Enthalpy profile *versus* reaction co-ordinate of HRP-A2-CO (——) and βHb–CO (– – –). S+L was taken as the reference state. A small M↔S+L barrier compared to the M→B barrier can explain the absence of an observable matrix process in HRP–CO.

40 cm^{-1} and indicates a co-operative transition involving many residues. By contrast, only a shift of the amide I band occurs at 20 K, where the ligand is still in the heme pocket. Thus binding involves two conformational transitions triggered by the transfer of the ligand into the heme pocket and bond formation with the iron. The high Gibbs energy of state B_1 also explains the absence of a matrix process. Figure 12 shows schematically the enthalpy of βHb–CO and HRP–CO *versus* the reaction co-ordinate of the ligand. If the barrier between M and S is much smaller than that between M and B, then M and S reach dynamic equilibrium and cannot be distinguished kinetically. The corresponding barriers in βHb have comparable heights, therefore a matrix process can be observed. Equation (1) indicates that the association rate λ_S is determined by a delicate balance of P_B and $\bar{k}_{BA}$. In a sequential model (Fig. 12) the two are not independent and λ_S is determined by the difference in Gibbs energy between the bottom of well S and the top of the barrier between B and A. Control of ligand binding can be achieved in two ways. (1) The transition state B→A can be exclusively varied through electronic or steric factors at the heme; level B remains constant. Examples are βHb–CO and Mb–CO, where P_B is similar but $\bar{k}_{BA}$ is very different (Doster *et al.*, 1982). (2) Level B can be changed without changing the difference between B and the B→A transition state. This situation seems to occur in Mb–CO and Mb–O_2, where $\bar{k}_{BA}$ is of similar magnitude but P_B is very different. A molecular realization could be conformational adjustments of the protein without affecting the ground and transition state of the ligand. A dramatic example is HRP–CO, which has a k_{BA} similar to βHb–CO but differs in P_B by 10^4 at 300 K.

One may wonder why P_B is so small in HRP. A possible explanation is the strong interaction of the distal His and the heme group in the absence of CO, which gives rise to an absorption band at 590 nm (Q_0). This band decreases in intensity with increasing pH (Teraoka & Kitagawa, 1981) and is absent in HRP–CO after photolysis at low temperatures. The ligand in the pocket seems to block the interaction.

5. Conclusion

The results of the present paper show that the general principles found in studies of simple heme proteins, such as myoglobin or the separated chains of hemoglobin, are useful to describe and classify the binding to a more complex protein, horseradish peroxidase. HRP, however, yields new insights into the mechanism of ligand binding, shows some new features, and poses new problems.

The new insights into the binding mechanism are connected to the small association rate for CO binding to HRP near 300 K. Our data show that the small λ_S is not the result of a slow reaction with the heme (Coletta *et al.*, 1986) but reflects the small partition coefficient P_B of CO in the heme pocket. The small value and the strong temperature dependence of P_B suggest a conformational transition associated with the transfer of a CO from the solvent to the heme pocket. This idea is supported by corresponding changes in the amide I band.

The new feature seen in HRP is the existence of two neatly separated pathways to binding as expressed in scheme S2. Of particular interest is the occurrence of the fast process I*, which is exponential in time, shows a remarkable temperature dependence, and occurs in only one pathway. While a similar process has already been observed in cm-cyt *c* and heme octapeptide, the appearance in HRP causes us to ask about its functional importance and its structural origin.

New problems are posed by the conformational transformation that presumably accompanies the motion of the CO molecule into the pocket and by the remarkable properties of the fast process I*. While we have some tentative explanations of these phenomena, much additional experimental and theoretical work will be needed to understand these features fully.

We are grateful to Tsunehisa Araiso and Rick Rutter for many discussions and for help with the sample preparation. We thank Lowell Hager and Edgar Lüscher for suggestions and support. The work was supported in part by the National Science Foundation under grant no. DMB82-09616, by the U.S. Department of Health & Human Services under grant no. GM18051, and by a NATO grant. W.D. acknowledges a grant by the Deutsche Forschungsgemeinschaft; S.F.B. acknowledges fellowships from Exxon and 3M Corporation.

References

Agmon, N. & Hopfield, J. J. (1983). *J. Chem. Phys.* **79**, 2042–2053.

Alben, J. O. & Bare, G. H. (1973). *Proc. Fed. Am. Soc. Exp. Biol.* **32**, 1586 (Abstract).

Alben, J. O., Beece, D., Bowne, S. F., Einstein, L., Frauenfelder, H., Good, D., Marden, M. C., Moh, P. P., Reinisch, L., Reynolds, A. H. & Yue, K. T. (1980). *Phys. Rev. Letters*, **44**, 1157–1163.

Alben, J. O., Beece, D., Bowne, S. F., Doster, W., Eisenstein, L., Frauenfelder, H., Good, D., McDonald, J. D., Marden, M. C., Moh, P. P., Reinisch, L., Reynolds, A. H., Shyamsunder, E. & Yue, K. T. (1982). *Proc. Nat. Acad. Sci., U.S.A.* **79**, 3744–3748.

Alberding, N., Austin, R. H., Beeson, K. W., Chan, S. S., Eisenstein, L., Frauenfelder, H. & Nordlund, T. M. (1976). *Science*, **192**, 1002–1004.

Alberding, N., Austin, R. H., Chan, S. S., Eisenstein, L., Frauenfelder, H., Good, D., Kaufmann, K., Marden, M., Nordlund, T., Reinisch, L., Reynolds, A. H., Sorensen, L. B., Wagner, G. C. & Yue, K. T. (1978). *Biophys. J.* **78**, 319–334.

Ansari, A., Berendzen, J., Bowne, S. F., Frauenfelder, H., Iben, I. E. T., Sauke, T. B., Shyamsunder, E. & Young, R. D. (1985). *Proc. Nat. Acad. Sci., U.S.A.* **82**, 5000–5004.

Ansari, A., Di Iorio, E. E., Dlott, D. D., Frauenfelder, H., Iben, I. E. T., Langer, P., Roder, H., Sauke, T. B. & Shyamsunder, E. (1986). *Biochemistry*, **25**, 3139–3146.

Austin, R. H., Beeson, K. W., Eisenstein, L., Frauenfelder, H. & Gunsalus, I. C. (1975). *Biochemistry*, **14**, 5355–5373.

Barlow, C. H., Ohlsson, P. & Paul, K. G. (1976). *Biochemistry*, **15**, 2225–2229.

Beece, D., Eisenstein, L., Frauenfelder, H., Good, D., Marden, M. C., Reinisch, L., Reynolds, A. H., Sorensen, L. B. & Yue, K. T. (1980). *Biochemistry*, **19**, 5147–5157.

Brill, H. S. (1966). In *Comprehensive Biochemistry* (Florkin, M. & Stotz, E., eds), vol. XIV, chap. 10, pp. 447–479, Elsevier, Amsterdam.

Brunori, M., Wilson, M. T. & Antonini, E. (1972). *J. Biol. Chem.* **247**, 6076–6081.

Campbell, B. N., Jr, Araiso, T., Reinisch, L., Yue, K. T. & Hager, L. P. (1982). *Biochemistry*, **21**, 4343–4349.

Colletta, M., Ascoli, F., Brunori, M. & Traylor, T. (1986). *J. Biol. Chem.* **261**, 9811–9814.

Dlott, D. D., Frauenfelder, H., Langer, P., Roder, H. & Di Iorio, E. E. (1983). *Proc. Nat. Acad. Sci., U.S.A.* **80**, 6239–6243.

Doster, W., Beece, B., Bowne, S., Di Iorio, E., Frauenfelder, H., Reinisch, L., Shyamsunder, E., Winterhalter, K. W. & Yue, K. T. (1982). *Biochemistry*, **21**, 4831–4839.

Dunford, H. B. & Araiso, T. (1979). *Biochem. Biophys. Res. Commun.* **89**, 764–768.

Evangelista-Kirkup, R., Smulevich, G. & Spiro, T. G. (1986). *Biochemistry*, **25**, 4420–4425.

Frauenfelder, H. (1979). In *Tunneling in Biological Systems*, pp. 627–649, Academic Press, New York.

Frauenfelder, H. (1983). *Structure & Dynamics: Nucleic Acids & Proteins*, (Clementi, E. & Sarma, R. H., eds), pp. 369–375, Adenine Press, New York.

Frauenfelder, H. & Wolynes, P. G. (1985). *Science*, **299**, 337–345.

Frauenfelder, H., Petsko, G. A. & Tsernoglou, D. (1979). *Nature (London)*, **280**, 558–563.

Goldanskii, V. (1979) *Nature (London)*, **279**, 109–115.

Hänggi, P., Grabert, H., Ingold, G. L. & Weiss, U. (1985). *Phys. Rev. Letters*, **55**, 761–764.

Hayashi, Y., Yamada, H. & Yamazaki, I. (1976). *Biochim. Biophys. Acta*, **427**, 608–616.

Jortner, J. & Ulstrup, J. (1979). *J. Amer. Chem. Soc.* **101**, 3744–3754.

Kertez, D., Antonini, E., Brunori, M., Wyman, J. & Zito, R. (1965). *Biochemistry*, **4**, 2672–2676.

LaMar, G. N., Chacko, V. P. & de Ropp, Y. S. (1982). In *The Biological Chemistry of Iron* (Dunford, H. B., Dolphin, D., Raymond, K. N. & Sicker, L., eds), pp. 357–373, D. Reidel Pub. Co., New York.

Landau, L. D. & Lifshitz, E. M. (1958). *Quantum Mechanics*, Pergamon Press, Oxford.

Martin, J. L., Migus, A., Prygurt, C., Lecarpentier, J., Astier, A. & Antonetti, A. (1984). In *Ultrafast Phenomena IV* (Auston, D. & Eisenthal, K., eds), pp. 447–451, Springer, New York.

Mincey, T. & Traylor, T. G. (1980). *J. Amer. Chem. Soc.* **191**, 756–766.

Perutz, M. F. (1979). *Annu. Rev. Biochem.* **48**, 327–386.

Provencher, S. W. & Dovi, V. G. (1979). *J. Biochem. Biophys. Methods*, **1**, 313–318.

Schmidt, W. R. & Reed, C. A. (1981). *J. Amer. Chem. Soc.* **104**, 2352–2356.

Shannon, L. M., Kuy, E. & Leu, J. Y. (1966). *J. Biol. Chem.* **241**, 2166–2172.

Stetzkowski, F., Banerjee, R., Marden, M. C., Beece, D. K., Bowne, S. F., Doster, W., Eisenstein, L., Frauenfelder, H., Reinisch, L., Shyamsunder, E. & Jung, C. (1985). *J. Biol. Chem.* **260**, 8803–8809.

Teraoka, I. & Kitagawa, I. (1981). *J. Biol. Chem.* **256**, 3969–3971.

Yamasaki, I., Araiso, T., Hayashi, J., Yamada, H. & Makino, R. (1978). *Advan. Biophys.* **11**, 249–281.

Young, R. D. (1984). *J. Chem. Phys.* **80**, 554–560.

Young, R. D. & Bowne, S. F. (1984). *J. Chem. Phys.* **81**, 3730–3737.

Edited by G. A. Gilbert